Biochemical and Biophysical Research Communications 417 (2012) 192–196

Contents lists available at SciVerse ScienceDirect

Biochemical and Biophysical Research Communications

journal homepage: www.elsevier.com/locate/ybbrc

Characterization and *in vitro* interaction study of a [NiFe] hydrogenase large subunit from the hyperthermophilic archaeon *Thermococcus kodakarensis* KOD1

Daisuke Sasaki [a], Satoshi Watanabe [a], Tamotsu Kanai [b], Haruyuki Atomi [b], Tadayuki Imanaka [c], Kunio Miki [a,*]

[a] Department of Chemistry, Graduate School of Science, Kyoto University, Sakyo-ku, Kyoto 606-8502, Japan
[b] Department of Synthetic Chemistry and Biological Chemistry, Graduate School of Engineering, Kyoto University, Katsura, Nishikyo-ku, Kyoto 615-8510, Japan
[c] Department of Biotechnology, College of Life Sciences, Ritsumeikan University, Noji-Higashi, Kusatsu, Shiga 525-8577, Japan

ARTICLE INFO

Article history:
Received 28 October 2011
Available online 25 November 2011

Keywords:
[NiFe] hydrogenase maturation
Thermococcus kodakarensis KOD1
The large subunit HyhL
HypA
HypC
In vitro interaction

ABSTRACT

The large subunit of the [NiFe] hydrogenases harbors a $NiFe(CN)_2(CO)$ cluster. Maturation proteins HypA, B, C, D, E, and F are required for the NiFe cluster biosynthesis. While the maturation machinery has been hitherto studied intensively, little is known about interactions between the Hyp proteins and the large subunit of the [NiFe] hydrogenase. In this study, we have purified and characterized the cytosolic [NiFe] hydrogenase large subunit HyhL from *Thermococcus kodakarensis* (*Tk*-HyhL). *Tk*-HyhL exists in equilibrium between monomeric and dimeric forms. *In vitro* interaction analyses showed that *Tk*-HyhL monomer forms a tight complex with *Tk*-HypA and weakly interacts with *Tk*-HypC. The expected ternary complex formation was not detected. These observations reflect a diversity in the mechanism of Ni insertion in [NiFe] hydrogenase maturation depending on the organism.

1. Introduction

Hydrogenases, which are widely distributed in bacteria, archaea, and some eukaryotes, catalyze the reversible formation and consumption of molecular hydrogen and contribute to energy metabolism [1]. The core structure of the [NiFe] hydrogenase consists of a large and a small subunit [2]. The large subunit carries a $NiFe(CN)_2(CO)$ cluster at the active site [3–5]. The NiFe cluster is not formed spontaneously. The biosynthesis/maturation of the [NiFe] hydrogenase proceeds through a stepwise process performed by HypA, HypB, HypC, HypD, HypE, and HypF as well as specific endopeptidases [6–8]. At present, the overall maturation process is proposed as follows; First, HypC, HypD, HypE and HypF catalyze the synthesis and incorporation of a Fe atom ligated with diatomic CN and CO [9–13]. Second, the Ni atom is inserted into the large subunit. HypA and HypB have been shown to play a major role in this step [14–19]. Finally, specific endopeptidases such as HycI cleave off the C-terminal tail of the large subunit to form an active "mature" enzyme followed by binding of the small subunit [20].

The functions of the Hyp proteins have been widely investigated in *Escherichia coli* and other bacteria [6]. Furthermore, we have performed structural and functional analyses of the Hyp proteins from the hyperthermophilic archaeon *Thermococcus kodakarensis* KOD1 [21–26]. These results have provided significant insights into the functional roles of each Hyp protein and the interactions among these Hyp proteins during the maturation process. However, little is known about how the Hyp proteins interact with the large subunit of the [NiFe] hydrogenase.

In this study, we have purified and characterized the cytosolic [NiFe] hydrogenase large subunit, HyhL from *T. kodakarensis* (*Tk*-HyhL). SEC analyses of mixtures containing *Tk*-HyhL and Hyp proteins indicate a tight complex formation between *Tk*-HyhL and *Tk*-HypA, and weak interaction between *Tk*-HyhL and *Tk*-HypC.

2. Materials and methods

2.1. Cloning, expression, and purification of the large subunit Tk-HyhL and maturation proteins Tk-HypA and Tk-HypC

The gene fragment encoding *Tk*-HyhL (TK2069, 428 a.a.) was amplified by PCR using the genomic DNA of *T. kodakarensis* KOD1 [21] with the forward primer 5′-gg**tctag**aaataattttgtttaactttaagaaggagatatacatatgaagaacgtttatctcccgatcaccg-3′ (*XbaI* site is shown in

Abbreviations: DTT, dithiothreitol; EDTA, ethylenediaminetetraacetic acid; ICP-AES, inductively coupled plasma-atomic emission spectrometry; IPTG, isopropyl-β-D-thiogalactopyranoside; PAGE, polyacrylamide gel electrophoresis; PCR, polymerase chain reaction; SEC, size exclusion chromatography; Tris, tris (hydroxymethyl)aminomethane.

* Corresponding author. Fax: +81 75 753 4032.
E-mail address: miki@kuchem.kyoto-u.ac.jp (K. Miki).

0006-291X/$ - see front matter © 2011 Elsevier Inc. All rights reserved.
doi:10.1016/j.bbrc.2011.11.083

bold) and the reverse primer 5′-cgc**ggatcc**gcaagcctcgccacgtgcac-3′ (*Bam*HI site is shown in bold). The amplified gene was inserted into pUC19 and, after confirming the sequences of the DNA fragments, the fragments were inserted into *Xba*I/*Bam*HI sites of pET21a(+) (hyhL_pET21a(+)) (Novagen). The *E. coli* Rosetta2(DE3)pLysS cells were transformed with hyhL_pET21a(+). The transformants were plated on Luria–Bertani (LB) agar plates containing 34 μg/mL of chloramphenicol and 100 μg/mL of ampicillin. Single colonies were separately picked and pre-cultured overnight at 37 °C. One percent (v/v) of pre-culture was inoculated into LB medium containing the same antibiotics as the LB agar plate. Expression of the recombinant protein was induced with 0.1 mM IPTG when cell density reached 0.4 at OD_{600} and was further incubated for 6 h at 37 °C. The harvested cell pellet was suspended in 50 mM Tris–HCl pH 8.0, 1 mM DTT, and the suspension was sonicated on ice with an output energy of 50 W for a total period of 150 s. The supernatant after centrifugation (30,000*g*, 30 min at 4 °C) was subjected to heat treatment at 80 °C for 10 min. The supernatant after centrifugation (30,000*g*, 30 min at 4 °C) was filtrated with a 0.22 μm pore filter (Millipore) and applied onto an anion exchange column (ResourceQ 6 mL, GE healthcare) equilibrated with 50 mM Tris–HCl pH 8.0, 1 mM DTT. Proteins were eluted with a 0–0.2 M linear gradient of NaCl. The eluted sample was concentrated and applied onto a size exclusion column (Superdex 200 10/300 GL 24 mL, GE healthcare) equilibrated with 20 mM Tris–HCl pH 8.0, 150 mM NaCl, 1 mM DTT at a flow rate of 0.5 mL/min. All chromatography procedures were performed at room temperature using ÄKTA explorer system (GE healthcare) under aerobic conditions.

Molecular mass of the purified sample was estimated with size exclusion chromatography (SEC) by comparing its retention volume to those of marker proteins (GE healthcare), aldolase (158 kDa), conalbumin (75 kDa), ovalbumin (44 kDa), carbonic anhydrase (29 kDa), ribonuclease A (17.3 kDa), and aprotinin (6.5 kDa). The K_{av} value is defined by the equation $K_{av} = (V_e - V_o)/(V_c - V_o)$, where V_e, V_o, and V_c are the elution, column void, and geometric column volumes, respectively. Oligomeric states were also confirmed by non-denaturing native-PAGE analysis. The quantitative and qualitative metal analyses of the sample were performed by ICP-AES using Optima 4300DV (PerkinElmer Inc., Waltham, MA, USA). UV–visible absorption spectrum was measured with NanoDrop 1000 (Thermo Fisher Scientific Inc., Wilmington, DE, USA).

To obtain metal free samples, EDTA was added to a final concentration of 10 mM in 50 mM Tris–HCl pH 8.0, 1 mM DTT prior to the cell sonication. EDTA was removed from the supernatant after heat-treatment by buffer exchange, and an anion exchange column chromatography was performed. $(NH_4)_2SO_4$ was added to a concentration of 1.5 M and the sample was applied onto a hydrophobic interaction column (Resource ISO 6 mL, GE healthcare) equilibrated with the same buffer. Proteins were eluted by a linear 1.5–0.3 M gradient of $(NH_4)_2SO_4$ at a flow rate of 6.0 mL/min. Size exclusion column chromatography was subsequently performed.

Expressions and purifications of *Tk*-HypA and *Tk*-HypC were performed as previously reported [24,26].

2.2. Interaction analysis between the large subunit and maturation protein

SEC analysis was carried out by using a size exclusion column (Superdex 200 10/300 GL 24 mL, GE healthcare) equilibrated with 20 mM Tris–HCl pH 8.0, 150 mM NaCl, 1 mM DTT. Protein mixture solutions (200 μl) containing the indicated amounts of *Tk*-HyhL and Hyp proteins were prepared by mixing the proteins and incubating overnight at room temperature. As for the mixtures containing three proteins, three kinds of the mixtures were prepared. Mixture I was prepared by adding *Tk*-HyhL to the mixture of *Tk*-HypA and *Tk*-HypC. Mixture II was prepared by adding *Tk*-HypC to the mixture of *Tk*-HypA and *Tk*-HyhL. Mixture III was prepared by adding *Tk*-HypA to the mixture of *Tk*-HypC and *Tk*-HyhL. These protein mixtures were subjected to heat-treatment at 85 °C for 15 min after overnight incubation. Complex formation was also confirmed by non-denaturing native-PAGE analysis.

3. Results

3.1. Characterization of the large subunit Tk-HyhL

T. kodakarensis possesses three distinct [NiFe] hydrogenase homologs on its genome; one encodes the cytosolic hydrogenase Hyh, another encodes the membrane-bound hydrogenase Mbh, whereas the third encodes a complex (Mbx) which does not exhibit hydrogenase activity and whole function is still not clear [22,23]. In this study, the cytosolic [NiFe] hydrogenase large subunit gene, the *Tk-hyhL* gene was cloned and the recombinant protein was successfully obtained using an *E. coli* expression system. An elution profile of the SEC of *Tk*-HyhL showed two major peaks (the *bold line* in Fig. 1A). The estimated molecular masses of *Tk*-HyhL proteins from these peaks are ~49 and ~94 kDa, which correspond to a monomer (48.3 kDa) and a dimer (96.6 kDa), respectively. When fractions containing only the monomer or dimer were individually reapplied to SEC, both monomeric and dimeric states were observed (data not shown). These results clearly show that *Tk*-HyhL is in slow equilibrium between monomeric and dimeric states. This monomer–dimer equilibrium was also observed by non-denaturing native-PAGE analysis (Fig. 1B). The equilibrium was partially shifted to the monomer when the sample was subjected to heat-treatment at 85 °C for 15 min and analyzed by SEC (data not shown).

The purified sample was brown in color. An ICP-AES analysis showed that the sample contained 0.23 Fe atoms per molecule of *Tk*-HyhL, along with a small amount of Zn and Ca atoms. No Ni atoms were detected. A UV–visible absorption spectrum of the *Tk*-HyhL solution showed broad absorption bands in 300–700 nm (the *bold line* in Fig. 1C). Monitoring at the wavelengths of 330 and 450 nm during SEC showed that both monomer and dimer contained Fe atoms (data not shown). An EDTA treated sample showed no absorption bands in the UV spectrum (the *broken line* in Fig. 1C), indicating that the Fe atom was completely removed from the sample. The EDTA treated sample also existed in the monomer–dimer equilibrium (data not shown).

3.2. In vitro interaction analysis between Tk-HyhL and Tk-HypA or Tk-HypC by SEC

When SEC was performed with a mixture of *Tk*-HypA and *Tk*-HyhL, the two proteins co-eluted as a new single peak (the *arrow* in Fig. 2A), indicating tight complex formation between these two proteins. The HyhL–HypA complex appeared at an elution volume of ~15.2 mL corresponding to an estimated molecular mass of ~63 kDa, which is consistent with the sum of the calculated molecular masses of *Tk*-HypA (15.7 kDa) and *Tk*-HyhL monomer (*Tk*-HyhLm) (48.3 kDa). These results indicate that *Tk*-HyhL forms a 1:1 binary complex with *Tk*-HypA. The EDTA treated sample of *Tk*-HyhL also formed a 1:1 complex with *Tk*-HypA (data not shown).

When a mixture of *Tk*-HypC and *Tk*-HyhL at an equal molar ratio was applied to the column, the peak height of *Tk*-HypC subtly decreased (the *gray arrow* in Fig. 2B) and the elution peak of *Tk*-HyhLm slightly shifted to a higher molecular mass (the *black arrow* in Fig. 2B). When the mixtures were prepared at a 2–3-fold molar excess of *Tk*-HypC, the peak height of *Tk*-HyhLm in SEC

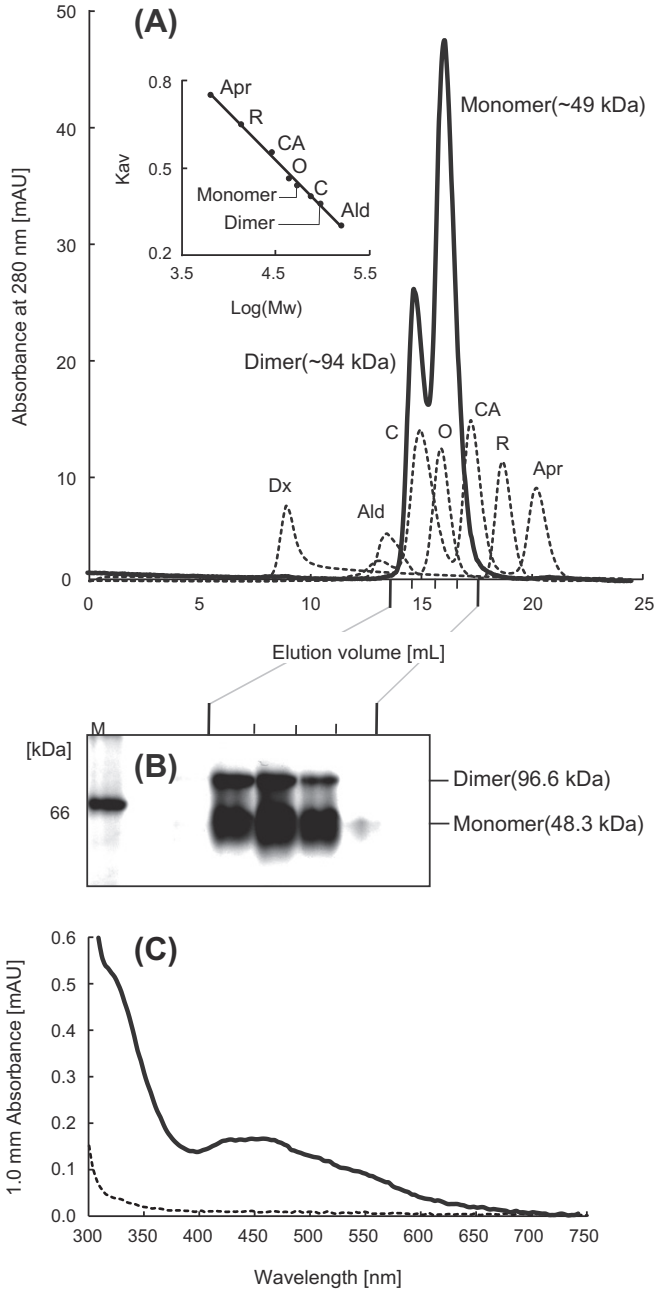

Fig. 1. Characterization of the [NiFe] hydrogenase large subunit HyhL from the *Thermococcus kodakarensis* KOD1 (*Tk*-HyhL). (A) Elution profiles from a superdex 200 10/300 GL column of *Tk*-HyhL. The molecular mass was estimated by the retention volume of the sample (*bold line*) compared with the protein markers (*broken lines*). (B) Non-denaturing native PAGE analysis (13% gel) of the fractions indicated in figure (A). Marker proteins (indicated by M) and the sample were analyzed. The lower and upper bands correspond to the positions of monomer (48.3 kDa) and dimer (96.6 kDa), respectively. (C) UV–visible absorption spectra of the original (*bold line*) and EDTA-treated (*broken line*) samples. Fe atom content of the original sample estimated by ICP-AES analysis is ~23%.

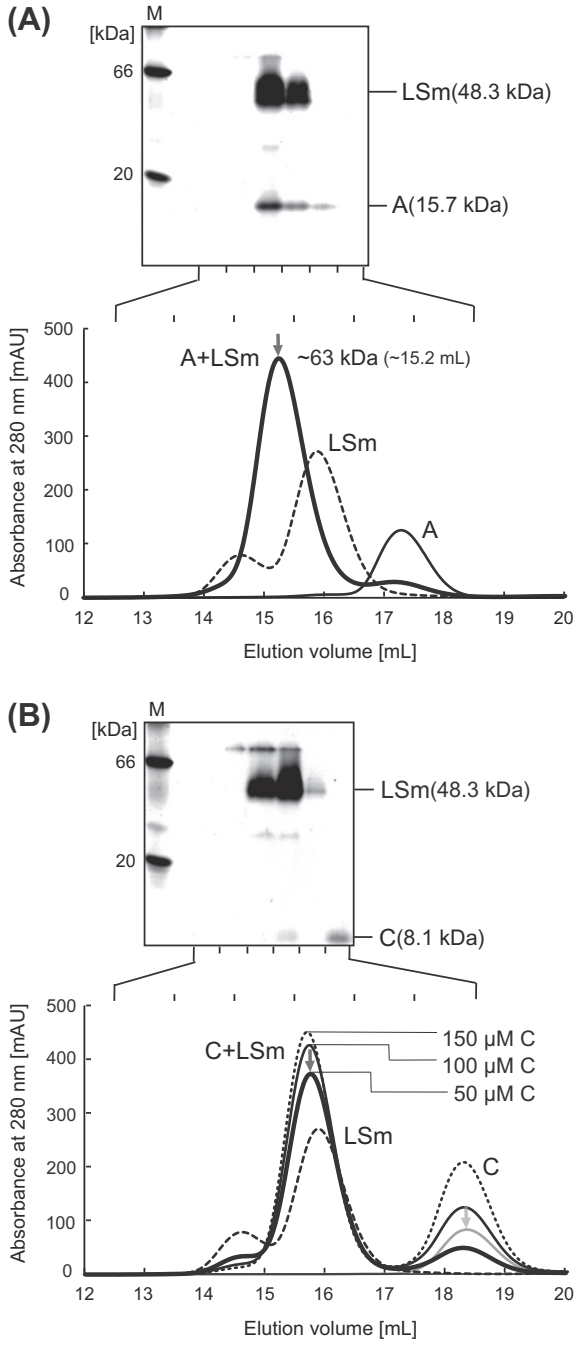

Fig. 2. *In vitro* interaction between *Tk*-HyhL and *Tk*-HypA and between *Tk*-HyhL and *Tk*-HypC. (A) SEC elution profiles of 50 μM *Tk*-HypA (*continuous line*), 50 μM *Tk*-HyhL (*broken line*) and a mixture containing 50 μM *Tk*-HypA and 50 μM *Tk*-HyhL (*bold line*). The estimated molecular mass of the protein–protein complex at the new peak (indicated by the *arrow*) indicates that *Tk*-HyhL monomer forms a 1:1 binary complex with *Tk*-HypA. Non-denaturing native-PAGE analysis (15% gel) of fractions in SEC of the HyhL–HypA mixture is shown in the upper panel. (B) SEC elution profiles of 50 μM *Tk*-HypC (*gray line*), 50 μM *Tk*-HyhL (*broken line*) and mixtures of 50 μM *Tk*-HyhL and 50–150 μM *Tk*-HypC (*bold, continuous, and dotted lines*). The SEC profile of the HyhL-HypC mixture suggests that *Tk*-HypC weakly interacts with *Tk*-HyhL. Non-denaturing native-PAGE analysis (15% gel) of fractions in SEC of the HyhL–HypC mixture is shown in the upper panel. LSm: the large subunit *Tk*-HyhL monomer; A and C: the maturation proteins *Tk*-HypA and *Tk*-HypC.

gradually increased. These observations suggest that *Tk*-HypC weakly interacts with *Tk*-HyhLm, most likely at a 1:1 M ratio.

3.3. In vitro interaction analysis between Tk-HyhL, Tk-HypA and Tk-HypC by SEC

We next examined whether *Tk*-HypA and *Tk*-HypC simultaneously interact with *Tk*-HyhL. When all three proteins were mixed together (mixture I) and applied to the column, a new peak appeared at an elution volume of ~15.2 mL (the *arrow* in Fig. 3), suggesting complex formation among these proteins. However, compared to the mixtures containing two components (*continuous and dotted lines* in Fig. 3), significant amounts of both *Tk*-HypA and

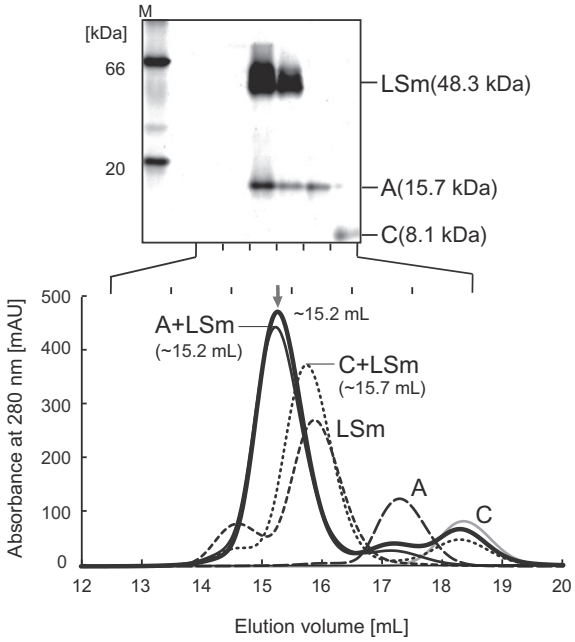

Fig. 3. Interaction analyses among *Tk*-HyhL, *Tk*-HypA and *Tk*-HypC. Elution profiles of 50 μM *Tk*-HypA (*broken line*), 50 μM *Tk*-HypC (*gray line*), 50 μM *Tk*-HyhL (*broken line*) and mixtures containing *Tk*-HypA, *Tk*-HypC and *Tk*-HyhL in equal molar ratio at a final concentration of 50 μM (*bold line*). The mixtures containing two components indicated by *bold lines* in Fig. 2 are shown by *continuous and dotted lines* in this Figure, respectively. Ternary complex formation was not observed under these conditions. LSm: the large subunit *Tk*-HyhL monomer; A and C: the maturation proteins *Tk*-HypA and *Tk*-HypC.

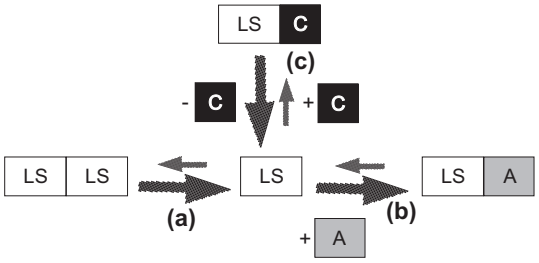

Fig. 4. *In vitro* interactions of the *T. kodakarensis* [NiFe] hydrogenase large subunit *Tk*-HyhL with maturation proteins *Tk*-HypA and *Tk*-HypC. (a) The equilibrium between *Tk*-HyhL monomer and dimer. (b) The 1:1 binary complex formation of *Tk*-HyhL monomer with *Tk*-HypA. (c) The probable 1:1 binary complex formation of *Tk*-HyhL monomer with *Tk*-HypC. LS: the large subunit *Tk*-HyhL; A and C: the maturation proteins *Tk*-HypA and *Tk*-HypC.

Tk-HypC remained in their free states. We further attempted to distinguish whether these interactions were sequential. Similar chromatography profiles were also observed when *Tk*-HypC (mixture II) or *Tk*-HypA (mixture III) was mixed with the other two proteins that were incubated in advance. The elution volume of the new peak (~15.2 mL) was faster than that of the HyhL–HypC complex (the *dotted line* in Fig. 3, ~15.7 mL) but slightly later than that of the HyhL–HypA complex (the *continuous line* in Fig. 3, ~15.2 mL). The peak height of the new peak was subtly higher than that of the HyhL–HypA complex probably because of the small overlap with the peak of the HyhL–HypC complex. Therefore, the new peak observed in SEC of the three component mixtures probably represents a mixture of the HyhL–HypA and HyhL–HypC binary complexes. The ternary complex formation among *Tk*-HypA, *Tk*-HypC and *Tk*-HyhL could not be detected under these conditions.

4. Discussion

In this study, we have characterized the [NiFe] hydrogenase large subunit HyhL from the hyperthermophilic archaeon *T. kodakarensis* KOD1 (*Tk*-HyhL) and investigated *in vitro* interactions with its maturation proteins *Tk*-HypA and *Tk*-HypC. The results from interaction analyses by SEC are summarized in Fig. 4.

The SEC analysis showed that the purified *Tk*-HyhL is in an equilibrium between monomer and dimer. Heat treatment at 85 °C affected the monomer–dimer equilibrium, suggesting that *Tk*-HyhL dominantly exists as a monomer rather than dimer under extreme growth environment around 80–95 °C (Fig. 4a).

The ICP-AES analysis showed that a portion of the *Tk*-HyhL sample contained a Fe atom, whereas Ni was not detected. The Fe atom is probably bound to the active site of the protein through conserved N- and C-terminal CXXC motifs [2], because *Tk*-HyhL has no cysteine residues other than those in the CXXC motif. It is very interesting why the Fe atom was inserted into *Tk*-HyhL without the assistance of the *T. kodakarensis* maturation proteins. The endogenous maturation system in *E. coli* might have contributed to the Fe atom insertion into the active site of *Tk*-HyhL [27].

Previous studies showed that, in the *E. coli* [NiFe] hydrogenase maturation, HypC remains associated with the large subunit (LS) after the incorporation of the $Fe(CN)_2(CO)$ ligand by the HypC–HypD complex and that HypA inserts the Ni atom into this precluster buried in the LS-HypC complex together with HypB and SlyD [6–8,28]. Interestingly, we have found that *Tk*-HyhL tightly interacts with *Tk*-HypA without *Tk*-HypC and the Fe ligand (Fig. 4b). On the other hand, *Tk*-HyhL weakly interacts with *Tk*-HypC (Fig. 4c). Furthermore, the expected ternary complex formation was not detected. SEC of the three-protein mixture suggests that the interaction site of the HyhL–HypA complex partially overlaps with that of the HyhL–HypC complex. These observations reflect a diversity in the mechanism of Ni insertion in [NiFe] hydrogenase maturation depending on the organism. For instance, three different types of HypB proteins are known according to the N-terminal region [29]. The gene of another Ni inserting protein SlyD has not been found in some species. The SlyD proteins identified so far have various length of the C-terminal metal-binding region [30]. In addition, the corresponding genes to the bacterial HypB and SlyD cannot be identified in *T. kodakarensis* and a number of species of archaea. Together with these genetic backgrounds of the maturation proteins involved in the Ni atom insertion, tight interaction between *Tk*-HypA and *Tk*-HyhL in the absence of *Tk*-HypC and the $Fe(CN)_2CO$ ligand implies that the Ni insertion step occurs independently of the incorporation of the Fe ligand in some kinds of archaea including *T. kodakarensis*. The $Fe(CN)_2CO$ ligand may be required for tight interaction between *Tk*-HypC and *Tk*-HyhL and for the ternary complex formation.

Acknowledgments

This work was partly supported by Grants-in-Aid for Scientific Research (A) (to KM) and by the Global COE program "International Center for Integrated Research and Advanced Education in Materials Science" (to DS) from the Ministry of Education, Culture, Sports, Science and Technology (MEXT) of Japan. The metal analysis of *Tk*-HyhL was performed by TORAY Research Center Inc.

References

[1] P.M. Vignais, B. Billoud, J. Meyer, Classification and phylogeny of hydrogenases, FEMS Microbiol Rev. 25 (2001) 455–501.
[2] A. Volbeda, M.H. Charon, C. Piras, E.C. Hatchikian, M. Frey, J.C. Fontecilla-Camps, Crystal structure of the nickel-iron hydrogenase from *Desulfovibrio gigas*, Nature 373 (1995) 580–587.

[3] R.P. Happe, W. Roseboom, A.J. Pierik, S.P. Albracht, K.A. Bagley, Biological activation of hydrogen, Nature 385 (1997) 126.
[4] A.J. Pierik, W. Roseboom, R.P. Happe, K.A. Bagley, S.P.J. Albracht, Carbon monoxide and cyanide as intrinsic ligands to iron in the active site of [NiFe]-hydrogenases $NiFe(CN)_2$ CO, biology's way to activate H_2, J. Biol. Chem. 274 (1999) 3331–3337.
[5] A. Volbeda, E. Garcin, C. Piras, A.L.D. Lacey, V.M. Fernandez, E.C. Hatchikian, M. Frey, J.C. Fontecilla-Camps, Structure of the [NiFe] hydrogenase active site: evidence for biologically uncommon Fe ligands, J. Am. Chem. Soc. 118 (1996) 12989–12996.
[6] A. Böck, P.W. King, M. Blokesch, M.C. Posewitz, Maturation of hydrogenases, Adv. Microb. Physiol. 51 (2006) 1–71.
[7] L. Forzi, R.G. Sawers, Maturation of [NiFe]-hydrogenases in *Escherichia coli*, Biometals 20 (2007) 565–578.
[8] M.R. Leach, D.B. Zamble, Metallocenter assembly of the hydrogenase enzymes, Curr. Opin. Chem. Biol. 11 (2007) 159–165.
[9] M. Blokesch, A. Paschos, A. Bauer, S. Reissmann, N. Drapal, A. Böck, Analysis of the transcarbamoylation-dehydration reaction catalyzed by the hydrogenase maturation proteins HypF and HypE, Eur. J. Biochem. 271 (2004) 3428–3436.
[10] M. Blokesch, A. Böck, Properties of the [NiFe]-hydrogenase maturation protein HypD, FEBS Lett. 580 (2006) 4065–4068.
[11] N. Drapal, A. Böck, Interaction of the hydrogenase accessory protein HypC with HycE, the large subunit of *Escherichia coli* hydrogenase 3 during enzyme maturation, Biochemistry 37 (1998) 2941–2948.
[12] S. Reissmann, E. Hochleitner, H. Wang, A. Paschos, F. Lottspeich, R.S. Glass, A. Böck, Taming of a poison: biosynthesis of the NiFe-hydrogenase cyanide ligands, Science 299 (2003) 1067–1070.
[13] M. Blokesch, S.P. Albracht, B.F. Matzanke, N.M. Drapal, A. Jacobi, A. Böck, The complex between hydrogenase-maturation proteins HypC and HypD is an intermediate in the supply of cyanide to the active site iron of [NiFe]-hydrogenases, J. Mol. Biol. 344 (2004) 155–167.
[14] T. Maier, A. Jacobi, M. Sauter, A. Böck, The product of the hypB gene, which is required for nickel incorporation into hydrogenases, is a novel guanine nucleotide-binding protein, J. Bacteriol. 175 (1993) 630–635.
[15] M. Hube, M. Blokesch, A. Böck, Network of hydrogenase maturation in *Escherichia coli*: role of accessory proteins HypA and HybF, J. Bacteriol. 184 (2002) 3879–3885.
[16] A. Atanassova, D.B. Zamble, *Escherichia coli* HypA is a zinc metalloprotein with a weak affinity for nickel, J. Bacteriol. 187 (2005) 4689–4697.
[17] N. Mehta, J.W. Olson, R.J. Maier, Characterization of *Helicobacter pylori* nickel metabolism accessory proteins needed for maturation of both urease and hydrogenase, J. Bacteriol. 185 (2003) 726–734.
[18] T. Maier, F. Lottspeich, A. Böck, GTP hydrolysis by HypB is essential for nickel insertion into hydrogenases of *Escherichia coli*, Eur. J. Biochem. 230 (1995) 133–138.
[19] J.W. Olson, N.S. Mehta, R.J. Maier, Requirement of nickel metabolism proteins HypA and HypB for full activity of both hydrogenase and urease in *Helicobacter pylori*, Mol. Microbiol. 39 (2001) 176–182.
[20] R. Rossmann, T. Maier, F. Lottspeich, A. Böck, Characterisation of a protease from *Escherichia coli* involved in hydrogenase maturation, Eur. J. Biochem. 227 (1995) 545–550.
[21] T. Fukui, H. Atomi, T. Kanai, R. Matsumi, S. Fujiwara, T. Imanaka, Complete genome sequence of the hyperthermophilic archaeon *Thermococcus kodakaraensis* KOD1 and comparison with *Pyrococcus* genomes, Genome Res. 15 (2005) 352–363.
[22] T. Kanai, S. Ito, T. Imanaka, Characterization of a cytosolic NiFe-hydrogenase from the hyperthermophilic archaeon *Thermococcus kodakaraensis* KOD1, J. Bacteriol. 185 (2003) 1705–1711.
[23] T. Kanai, R. Matsuoka, H. Beppu, A. Nakajima, Y. Okada, H. Atomi, T. Imanaka, Distinct physiological roles of the three [NiFe]-hydrogenase orthologs in the hyperthermophilic archaeon *Thermococcus kodakarensis*, J. Bacteriol. 193 (2011) 3109–3116.
[24] S. Watanabe, T. Arai, R. Matsumi, H. Atomi, T. Imanaka, K. Miki, Crystal structure of HypA, a nickel-binding metallochaperone for [NiFe] hydrogenase maturation, J. Mol. Biol. 394 (2009) 448–459.
[25] S. Watanabe, R. Matsumi, T. Arai, H. Atomi, T. Imanaka, K. Miki, Crystal structures of [NiFe] hydrogenase maturation proteins HypC, HypD, and HypE: insights into cyanation reaction by thiol redox signaling, Mol. Cell 27 (2007) 29–40.
[26] S. Watanabe, R. Matsumi, H. Atomi, T. Imanaka, K. Miki, Crystallization and preliminary X-ray crystallographic studies of the [NiFe] hydrogenase maturation proteins HypC and HypD, Acta Crystallogr. Sect. F Struct. Biol. Cryst. Commun. 63 (2007) 538–541.
[27] J. Sun, R.C. Hopkins, F.E. Jenney, P.M. McTernan, M.W. Adams, Heterologous expression and maturation of an NADP-dependent [NiFe]-hydrogenase: a key enzyme in biofuel production, PLoS One 5 (2010) e10526.
[28] M. Blokesch, A. Böck, Maturation of [NiFe]-hydrogenases in *Escherichia coli*: the HypC cycle, J. Mol. Biol. 324 (2002) 287–296.
[29] R. Gasper, A. Scrima, A. Wittinghofer, Structural insights into HypB, a GTP-binding protein that regulates metal binding, J. Biol. Chem. 281 (2006) 27492–27502.
[30] H. Kaluarachchi, D.E. Sutherland, A. Young, I.J. Pickering, M.J. Stillman, D.B. Zamble, The Ni(II)-binding properties of the metallochaperone SlyD, J. Am. Chem. Soc. 131 (2009) 18489–18500.